Three-Dimensional Analyses of Excavation Support System for the Stata Center Basement on the MIT Campus

Citation: Orazalin, Zhandos Y., Andrew J. Whittle, and Matthew B. Olsen. "Three-Dimensional Analyses of Excavation Support System for the Stata Center Basement on the MIT Campus." Journal of Geotechnical and Geoenvironmental Engineering 141, no. 7 (July 2015): 05015001.

As Published: http://dx.doi.org/10.1061/(ASCE)GT.1943-5606.0001326

Publisher: American Society of Civil Engineers (ASCE)

Persistent URL: http://hdl.handle.net/1721.1/102384

Version: Author's final manuscript: final author's manuscript post peer review, without publisher's formatting or copy editing

THREE-DIMENSIONAL ANALYSES OF EXCAVATION SUPPORT SYSTEM FOR STATA CENTER BASEMENT ON MIT CAMPUS

by

Zhandos Y. Orazalin[1], Andrew J. Whittle[2] M.ASCE, & Matthew B. Olsen[3]

ABSTRACT

The basement of the Stata Center building on the MIT campus required 12.8m deep excavations covering a large open-plan site and underlain by more than 25m of lightly overconsolidated Boston Blue Clay. The excavations were supported by a floating, perimeter diaphragm and braced with a system of internal corner struts, rakers and tieback anchors. The project involved a complex sequence of berms, access ramps and phased construction of the concrete mat foundation. One of the key goals of the design was to limit ground movements in order to prevent damage to adjacent structures including the Alumni Pool building, which was founded on shallow caissons and located less than 1.5m from the south wall. Lateral wall movements and building settlements were closely monitored throughout construction, while photos from a network of webcams located around the open-plan site provide a detailed time history of the construction processes. This paper describes the development of a comprehensive 3D finite element model for the Stata Center basement excavation, which has been enabled by recent advances in available Plaxis 3D software including efficient multicore iterative solving capabilities, importing of geometric data from CAD files, and use of embedded pile elements to represent tieback anchors. The analyses highlight the effects of the 3D excavation and support geometry on wall and ground movements. The base case results using a simple elasto-plastic (MC) soil model with undrained conditions in the clay are generally in very good agreement with measured performance. The effects of refined constitutive modeling and partial drainage within the clay have a secondary role on numerical predictions for this project.

[1] Ph.D student, Massachusetts Institute of Technology, Cambridge, MA
[2] Professor of Civil & Environmental Engineering, Massachusetts Institute of Technology, Cambridge, MA
[3] Senior Geotechnical Engineer, AMEC Environment & Infrastructure, Durham, NC

KEYWORDS:

Braced excavation, diaphragm wall, ground deformations, field measurements, finite element analysis

INTRODUCTION

It is more than 10 years since the completion of the Ray and Maria Stata Center on the MIT Campus. The building (which houses two large computer science labs, the Departments of Linguistics and Philosophy, and is the current home of the World Wide Web Consortium) was designed by the renowned architect Frank Gehry and is located on the site formerly occupied by the famed Radiation Laboratory (Building 20, demolished in 1999). The Stata Center includes two levels of underground parking and building service facilities that required 12.8m deep excavations over a large, open-plan area (approx. 100m x 120m). Figure 1 shows the layout of the site and proximity to existing buildings. The excavation was supported by a perimeter diaphragm wall (part of the permanent structure) and braced using corner struts (2 levels) and tieback anchors (3 levels) along three sides of the excavation pit, and by raker beams (2 levels) on the North side fronting Vassar Street. The construction involved a complex sequence of excavations, support berms and access ramps, with construction of the base slab progressing generally from the South East to the North-West corner of the site. Olsen (2001) documented the actual construction sequence in exquisite detail based on field records, photographs and continuous videos from a network of 11 webcams mounted on adjacent buildings (Rodriguez, 2000). Figure 2 illustrates the excavation and support system at four selected stages of construction.

One of the main design concerns was to limit ground movements in order to prevent damage to adjacent structures including the Alumni Pool (Building 57; Fig. 1, Table 1), which was founded on shallow caissons and located less than 1.5m from the south wall (and was itself the subject of a case study paper by Taylor, 1944). Lateral wall deflections were monitored closely by a set of 11 inclinometers (installed through the diaphragm wall panels to bedrock), together with regular surveys of vertical movements at 150 reference points on the adjacent buildings and roadway. The measured performance was described in detail by Olsen (2001) and summarized by Hewitt et al. (2003).

Although it is readily apparent that the selected bracing system and excavation sequence will influence the distribution and magnitude of deformations around the perimeter of the site, predictions of performance at the time were limited to simplified 2D finite element models (plane strain, half-sections) that are assumed to generate worst-case scenarios for wall deflections and ground

deformations. Indeed, the complexity of the excavation process and structural supports present a significant modeling challenge, and exceeding the computational capabilities of finite element codes available at the time. There are only a relatively small number of published case studies detailing comparisons between 3D finite element models and the measured performance of excavation support systems. The papers by Ou et al. (1996), Lee et al. (1998) and Finno et al. (2007) all focus on 3D deformations around the corner of an excavation pit. Yeow et al. (2006) described the use of a 3D finite element model (using LS-Dyna^{TM}) to understand the effects of ground movements associated with the design of the new terminus for the Channel Tunnel Rail Link beneath St Pancras station in London. Their analyses use the BRICK model (Simpson, 1992) to describe non-linear stress-strain properties of London clay, but gives no comparisons with measured behavior. Lee et al. (2011) describe back-analyses of the collapse of the Nicoll Highway using undrained, total stress analyses (ABAQUS^{TM} with Mohr-Coulomb soil models). They show the progressive splitting of diaphragm wall panels associated with 30m deep excavations through a deep relict channel filled with soft marine clay, but the validation is limited to one instrumented section. Dong et al. (2013) are among the first to compare comprehensive 3D finite element analyses (using ABAQUS^{TM}) and monitoring data for the top-down construction of the basement for the Shanghai Xingye bank. Their analyses include a multi-yield surface model (Houlsby, 1999) for non-linear undrained stress-strain properties of Shanghai clay and focus on effects of thermal shrinkage of the cast in-situ floor slabs.

This paper describes the development of a 3D finite element model for the basement of the Stata Center. The analyses are performed using the Plaxis 3D-2012^{TM} program (Brinkgreve et al., 2012) and make extensive use of specific capabilities of this software, notably the introduction of embedded pile elements to represent tieback anchors. The program is able to simulate coupled flow and deformation within the soil mass and hence, can represent partial drainage within the soil mass, while advanced effective stress soil models such as MIT-E3 (Whittle and Kavvadas, 1994) are integrated within the program kernel. Numerical simulations have been carried out to investigate the relative importance of different modeling assumptions on predictions of excavation performance, as observed in comparisons with the field monitoring data.

PROJECT DESCRIPTION

The project site is located at the Northeastern part of the MIT campus, an area of tidal marshes that were filled in the late 1800's and later used for university athletic fields. The only prior construction on the site was Building 20, a three-story above-grade, wooden structure that originally housed the Radiation Laboratory during the Second World War. Figure 3 illustrates a typical North-South cross-section across the basement of the Stata Center. The ground surface is approximately level at El. 6.4m. Within the footprint of the site, the subsurface stratigraphy was determined from a series of 10 seismic piezocone penetration tests and two deep borings (B-101, B-102) that extended up to 40m below the ground surface (into the underlying bedrock). Extended cross-sections were developed using a database of borings from other buildings on the campus. The typical profile includes up to 10m of surficial units comprising granular fill, organics (silt and peat) and marine sand overlying a deep unit of Boston Blue Clay (BBC). The upper surface of the clay is almost level (average El. -2.4±1.2m) across the site and beyond. Although the clay varies in thickness from 18 to 30m in this area of the campus, the current analyses assume a constant thickness (with base at El. -29m) that corresponds closely to conditions spanning from the NW to SE corner of the Stata Center site. The clay is underlain by a continuous drape of glacial till, principally comprising dense sands and gravels with an average thickness of 4.6m. Weathered bedrock (Cambridge argillite) is located at El. -30 to -34m.

The groundwater table at the site is at El. 4.6m, corresponding closely to the water level in the Charles River, and data from piezometers installed in the clay show that pore pressures are hydrostatic through the soil profile.

There is little site-specific data on the engineering properties of the surficial soils. The fill ranges in thickness 4±1.6m with an average SPT blow count, N = 15bpf. The organic layer has quite variable thickness (1.2 – 6.7m) and includes fine sand layers, while the marine sand is a dense, fine to medium sand with SPT, N = 26±6 bpf.

Detailed investigations of the properties of Boston Blue Clay at the site were motivated in part by poor performance of excavation support systems for Building 68 (cf. Fig. 1; Berman et al., 1993) and by the close proximity of adjacent buildings. A series of 20 1-D CRS consolidation tests were

performed on high quality tube samples from the two deep borings, while the in situ shear strength was evaluated from a series of 10 piezocone tests. Laboratory measurements of pre-consolidation pressure show that the BBC is overconsolidated over the entire depth, Figure 4b. The unit can be sub-divided into an upper crust in which the OCR ranges from a maximum, OCR = 4.5 - 5.0 at the top of the clay to OCR ≈ 1.5 at El. -16m. The OCR is approximately constant below this elevation. These findings are consistent with measurements reported for Building 68 (Berman et al., 1993) but differ significantly from other test sites in South and East Boston as reported by Ladd et al. (1999) and Ladd and DeGroot (2003). Figure 4c shows that there is very good agreement between profiles of average undrained shear strength estimated from i) the stress history through the well known SHANSEP equation with input parameters S = 0.205 m = 0.77 (equivalent to s_{uDSS}; Ladd et al., 1999); and 2) the net piezocone tip resistance $[q_T-s_{v0}]/N_{kt}$, using a cone resistance factor, N_{kt} = 19 as recommended by Berman et al. (1993). The undrained shear strength ranges from a minimum value, s_u = 60kPa at El. -16m to a maximum, $s_u \approx$ 90kPa at the base of the clay. Values of in situ hydraulic conductivity were obtained from CRS tests, Figure 4d, and show minimal variation with depth with an average value, $k_v = 4x10^{-5}$ m/day.

The excavation is supported by a 0.76m thick reinforced concrete diaphragm wall that serves as the exterior basement wall of the final structure and extends to a total depth of 21.6m (i.e., the toe of the wall floats within the clay at El. -15.3m). The wall comprises 65 panels and was constructed with pre-installed sleeves for subsequent installation of tieback anchors, and bearing plates for the corner braces and rakers. Three rows of temporary tieback anchors were installed along the mid-sections of the East, South and West walls (Fig. 1). Each anchor was drilled at an inclination of 20°, with bonded lengths ranging from 12m to 15m located in the marine sand and upper BBC, at an average horizontal spacing of 1.5m. The tiebacks were preloaded to 50% of the estimated design loads, corresponding to forces in the range, 500-570 kN. The wall and bracing system were designed using the finite element program ANSYS (Hewitt & Haley, 2003). Along the Southern wall there was some interference between the installation tiebacks (Fig. 5a) and caisson foundations for Building 57 affecting 10-15% of the 135

anchors (as indicated in Fig. 3). Hewitt et al. (2003) report that 35% of the third level tiebacks were post-grouted more than 3 times in order to achieve the required design capacity.

The City of Cambridge prohibited tieback installation beneath Vassar Street. Hence, the excavation support system for the North wall comprises 8 pairs of 91cm diameter pipe strut raker beams (spaced 7.6m apart), that were preloaded against kicker blocks embedded in the 1.2m thick concrete mat foundation, Figure 5b. A soil berm was left in front of the north wall during raker installation and preload forces were set at 50% of the expected design loads. The upper raker beams were insulated to reduce thermal expansion after berm removal. Two levels of preloaded pipe struts were used to brace the four corners of the excavation. Tables 2-4 give full details of the geometry, properties and preloading of the bracing elements, while Figure 6 summarizes the chronology of support installation (showing concurrent activities at different parts of the site). It should be noted that Ukritchon et al. (2003) reported 2D stability analyses for the North wall with a safety factor, FS = 1.70 – 2.05, at the final excavated grade.

One of the principal concerns in the design of the excavation support system was the magnitude of associated ground movements and their impacts on the adjacent buildings. The initial evaluation of Buildings 57 and 36 led to a maximum allowable settlement (and lateral wall deflection) of 38mm (Olsen, 2001). Movements were monitored closely during construction through a series of 11 inclinometers installed within the diaphragm wall panels (and extending into the underlying bedrock), Figure 1, and through surveys involving approximately 150 surface reference points mainly located on buildings and along Vassar St. Additional information included measurements of pore pressures and subsurface vertical movements from 12 vibrating wire piezometers and 5 magnet extensometers installed within boreholes below the base of the excavation (two locations shown in Fig. 1).

DEVELOPMENT OF 3D FINITE ELEMENT MODEL

The construction of the Stata Center basement involves a complex sequence of excavation (with access ramps, berms etc), installation of bracing elements and floor slab construction. Olsen (2001)

developed a series of 3D geometric models to represent the construction process by reconciling daily field reports, photographs and time-lapse of the project. Figure 7 illustrates the process of converting the geometric information into Phases used in the development of the 3D finite element model. Project data from project drawings were initially used to construct a CAD model of the support system. This information was then used to create a base case model within Plaxis 3D. The excavated surface geometry is obtained from models reported by Olsen (2001) that are converted into a set of tetrahedral elements using mesh tessellation operators in the CAD program. These are then imported into Plaxis 3D as soil clusters that represent the excavation process as a series of 36 'staged construction' steps in the finite element model. Figure 7 shows that the resulting finite element model represents a close approximation to the original geometric model (Fig. 7d vs 7b).

The overall finite element model extends laterally beyond the footprint of the excavation to a distance of 150-170m in all directions and vertically to the base of the glacial till. Pore pressures are assumed to remain hydrostatic in the underlying, more permeable till and around all far field boundaries. The model represents the foundation of the Alumni Pool (Building 57) as a surcharge load acting at the tip of the caisson foundations (Table 1), but does not include the foundations of other buildings. It is assumed that loads from spread footings of the former Building 20 have negligible effect on soil stresses and properties at the site. The soil is represented by 10-noded tetrahedral elements with second order interpolation or displacements and full integration of element stiffness. The current FE model represents the soil mass using approximately 11200 elements and includes more than 520,000 degrees of freedom.

The FE model represents the diaphragm wall using elastic plate elements and assumes isotropic stiffness properties of the wall representing the bending stiffness of the uncracked wall section. We have checked these assumptions through parametric analyses and found minimal effects of reducing the wall bending stiffness (to represent cracked section properties) or introducing equivalent anisotropoic properties to represent the response of the jointed diaphragm wall panels (cf. Zdravkovic et al., 2005). Plate elements have also been used for the base slab (it should be noted that the rotational fixity/moment connection between the wall and base slab has minimal influence on the predictions

presented in this paper), while the rakers and corner braces are represent by 3-noded line elements with axial stiffness and preloads listed in Table 4. The fixed lengths of the tieback anchors are represented by 'embedded pile' elements within the Plaxis 3D program (based on the formulation proposed by Sadek & Shahrour, 2004). The embedded piles comprise beam elements that can be placed at arbitrary orientation within the soil mass/clusters and are connected to the soil through non-linear interface elements that control the limiting shaft (and tip) resistance between the pile and soil. In practice, tieback anchors are designed and tested in the field to ensure that first yielding occurs in the steel tendon. The current analyses assume a minimum shaft adhesion, f_s = 40kPa (equivalent to a shaft resistance, Q_s = 760kN, for the shortest anchors) to ensure no slippage along the fixed anchor lengths (i.e., displacements of the fixed anchors are controlled by the shear strength of the embedding soil layers). The tiebacks are activated in sets with prescribed lock-off loads listed in Table 2 (the field data show very small variations in lock-off loads among individual anchors in each row). Figure 6 shows the correspondence between the 35 analysis Phases ultimately used in the FE model with the actual construction dates and sequencing of support installation.

Tables 5 and 6 summarize the key input parameters and models used to describe soil behavior in the finite element model. The upper soil units (fill, organics and marine) and underlying glacial till are all described using a simple linear elastic-perfectly plastic soil model (Mohr-Coulomb; MC) with input parameters based on SPT correlations and prior empirical experience from projects in the local area (Table 5). The Boston Blue Clay has been modeled using three approaches:

A. Undrained conditions using the MC model (referred to as Method B after COI, 2005; Whittle & Davies, 2006). The layer is subdivided into two units, each with undrained shear strength varying linearly with elevation (i.e., matching the undrained strength profile shown in Fig. 4c).

B. Undrained conditions using the MIT-E3 effective stress soil model (Whittle & Kavvadas, 1994). MIT-E3 is a generalized effective stress soil model that describes rate independent behavior of normally and moderately overconsolidated clays. The model describes a number of important aspects of soil behavior including small strain non-linearity and anisotropic stress-strain-strength properties and has been validated through extensive comparisons between computed and

measured effective stress-strain-strength behavior in a variety of laboratory shear modes. Appendix A summarizes the input material constants used for the MIT-E3 model (unchanged from Whittle et al., 1994); while Table 6 shows the initial values of the stress history state variables assumed in the current calculations (5 sub units with specified OCR). These parameters have been chosen, such that MIT-E3 replicates closely the undrained shear strength profile in Figure 4c in the undrained direct simple shear mode (s_{uDSS}).

C. Partially drained conditions using the MIT-E3 soil model. This case uses the same model input parameters and state variable, but simulates consolidation using the average hydraulic conductivity shown in Table 6 with time steps for the construction phases shown in Figure 6.

All three cases assume horizontal soil layers with initial stress defined by K_0 conditions (Table 3), and hydrostatic pore pressures, with groundwater table at El. 4.6m.

RESULTS AND INTERPRETATION

Figure 8 illustrates predictions of wall deflections and surface settlements for analyses Case A at three key stages of the excavation process. The results show clearly the effects of the very stiff corner bracing in constrain the deformation mode shapes of the diaphragm wall. Maximum wall deflections, δ_w = 76mm, occurs at the central section of the South wall. Similar first order mode shapes occur on the East and West walls, while the raker support system and kink in wall alignment at the center of the North wall (cf. Fig. 1) produce a higher order mode shape with maximum deflections, δ_w = 50mm, occurring at the quarter points along the wall. Surface settlements are correlated with the wall deflections. The Case A predictions show maximum surface settlements δ_v = 32mm close to the center of the south wall (i.e., slightly smaller than the allowable settlement) while smaller settlements occur around the East, North and West walls.

Figure 9 presents comparisons between the computed and measured wall deflections for the 11 inclinometers located around the perimeter (Fig. 1) at 4 stages of construction (spanning the period from mid January to June 2001 and corresponding to the geometric configurations shown in Fig. 2).

The inclinometers can be sub-divided into sections where the wall is supported by tieback anchors (SC-10, SC-08, SC-07, SC-04), corner bracing (SC-11, SC-09, SC-06, SC-05 and SC-03) and raker supports (SC-02, SC-01). The measured data show some important trends:

1. Maximum wall deflections typically occur at or slightly below the excavated grade at all points around the perimeter. The largest wall deflections occurred at the center of the South wall, δ_w = 80mm (SC-07) while the adjacent inclinometers show δ_w = 60±4mm (SC-06, SC-08). In contrast, inclinometers SC-01, SC-03 on the North wall measure larger wall deflections (δ_w = 74mm) than the central location SC-02 (δ_w = 50mm).

2. Toe movements along the South, East and West walls are typically 80-85% of the maximum wall movements, but constitute a much smaller fraction of the full range measured in the North wall (toe movements, 30-32mm for SC-01, SC-02, SC-03).

3. The tieback support system is only partially successful in controlling wall deflections. For example, inclinometer SC-07 shows significant inward translation over the full height of the wall ($\Delta\delta_{\Gamma}$ = 15-25mm) after Stage 21 when all three rows of tieback anchors are installed. These results imply that the fixed anchors are located within the zone of ground movement induced by excavations during this time period. Similar results can be seen for inclinometers located in other sections supported by tiebacks (SC-08, SC-04, SC-10). In contrast, the pre-loaded corner bracing is effective in constraining movements in the upper part of the wall (seen through comparisons of SC-09, SC-11 vs SC-10).

4. Three inclinometers (SC-11, SC-03 and SC-09) measure negative displacements occurring near the top of the diaphragm wall panels. This behavior almost certainly reflects low stiffness of the superficial soil layers, most likely due to loss of ground occurring during slurry trenching operations. These movements occur prior to inclinometer installation and are difficult to detect as they can occur beneath the guide wall. There are no detailed records of ground movements occurring during this phase of construction (July – November 2000). However, the trenching contractor did use shorter wall panels on the South wall to reduce potential ground losses in front of Building 57.

In general, the patterns of measured wall deflections are very well described by the base case finite element model, Case A. The Case A results are within 5-10mm of the measured maximum and toe deflections of the diaphragm wall at the end of construction (Phase 35), with the noted exception of conditions at the NW and NE corners of the site (SC-11, SC-01 and SC-03), where measured maximum wall deflections are 20mm higher than the numerical predictions. The Case A results are in particularly good agreement with wall deflections along the tieback-supported South wall and in excellent agreement with maximum deflections at the center of the raker-supported North wall. Inward movements measured by SC-07 from Phase 29-35 (6-8mm) occurred after construction of the mat foundation, and reflect either compression of the slab during curing or imperfect contact between the slab and diaphragm wall, neither of which is captured in the current numerical analyses.

The Case B analysis using the MIT-E3 soil model predicts slightly smaller wall deflections at most locations. In most instances, the differences between Cases A and B are less than 5mm. This is a surprising result given the large difference in stiffness properties represented by the MC and MIT-E3 soil model. The current analyses have used MC input parameters based on extensive prior empirical studies for excavations in the local area. In contrast, anisotropic stiffness properties for MIT-E3 were based on laboratory tests on resedimented clays (Appendix A, after Whittle et al. 1994). Figure 10a compares the elemental response computed by the two models in the undrained direct simple shear mode for mid-depth locations within the Upper (UC) and Lower (LC) units of BBC. The MIT-E3 model predicts non-linear stress-strain properties during shearing but matches closely the undrained shear strength assumed by MC (as explained above for Fig. 4c). Figure 10b shows that MIT-E3 generates much higher shear stiffness than MC at small shear strain levels ($\gamma < 0.01\%$; ultimately converging to a value, G_{max}, that controls elastic shear wave propagation). The stiffness properties of the two models can be compared in the finite element analyses by considering average levels of shear strains mobilized within the clay towards the end of the excavation process. Results obtained from FE analysis Cases A and B at locations corresponding to the middle of each wall show shear strains in the range 0.07 – 0.1% in the UC and 0.1 – 0.3% in the LC. At these levels of shear strain the two soil models (MC and MIT-E3) describe very similar secant stiffness properties and hence, it is not

surprising that the computed wall deflections are similar. The close correspondence between the two models is largely serendipitous and reflects the geometry (depth to till, excavation depth), and overconsolidated stress history in the clay at this site. Larger differences have been found in other case studies (with floating wall support systems) carried out at sites in South Boston that were characterized by deeper excavations (lower factor of safety against basal stability) and underlain by normally consolidated BBC (Jen, 1998; Corral, 2013).

It is likely that MIT-E3 overestimates the in situ shear stiffness of the BBC at the Stata Center site as the model input parameters were based on model calibrations using resedimented clay. Seismic piezocone tests at the site (Haley & Aldrich, 2000) found average shear wave velocity, v_s = 200±10 m/s through the depth of the BBC, implying an average small strain shear stiffness, G_{max}/σ'_{v0} = 380 (for piezocones P4 and P5 as reported in Fig. 4). This is significantly lower the small strain stiffness assumed by MIT-E3 with input parameters reported by Whittle et al., 1994) where $G_{max}/\sigma'_{v0} \approx 800$ for the average OCR used in the current analyses. This result may explain why the MIT-E3 soil model tends to underestimate the measured wall deflections shown in Figure 9.

The results at SC-07 and SC-06 (Fig. 9) show that the numerical analyses are capable of describing accurately the measured wall deflections throughout the construction process, from initial cantilever deflections through final support conditions (with three levels of tiebacks and completion of the base slab). In comparison, the measured responses in the NE and NW corners (SC-11, SC-01 and SC-03) show negative deflections at the top of the wall, larger inward deflection at the final excavated grade elevation and hence, significantly greater flexure of the wall than the numerical analyses. There are a range of possible factors influencing these results including approximations in the representation of stratigraphy, initial ground surface and top of wall elevations used in the FE models; overestimation of the wall bending stiffness or rotational stiffness at joints between diaphragm wall panels. We have performed further analyses to investigate some of these factors, but consider that the most likely causes are ground loss during construction of the wall panels and lack of preloading of 2nd level corner bracing prior to final excavation of berms in the NE corner.

Figure 11 summarizes the effects of partial drainage within the underlying BBC unit by comparing computed wall deflections from analyses Cases B and C. The effects of partial drainage are controlled by the hydraulic conductivity of the clay (Fig. 4d) and its stiffness properties (described by the MIT-E3 model), by the assumption of free draining boundary conditions above and below the clay, and by the timeframe of construction (approximately 200 days). The results in Figure 11 show that partial drainage Case C generates slightly smaller wall deflections than the undrained analysis, Case B. The differences in magnitude range from 1-2mm in the corners to 10mm at the center of the South wall. The results confirm that partial drainage has only a small effect on the computed wall deflections and that the behavior can be well approximated by conventional undrained assumptions.

Ground surface and building settlements were monitored through optical surveys of reference points. Figure 12 compares the measured and computed settlements at the end of the excavation along along axes orthogonal to the four walls . Only a subset of the reference points close to the diaphragm wall have been included in this figure as most of the data are affected by the stiffness of the adjacent buildings that has not been simulated in the analyses. The results show small differences in behavior computed using Cases A and B, again confirming that stiffness properties of the overconsolidated BBC layer have only a small influence on the ground response for this project. The computed results show maximum surface settlements occurring at ~15-20m from the wall, with smaller settlements for the East and West walls (δ_v = 17-20mm) compared to the North and South walls (δ_v = 25-29mm and 31-35mm respectively). These computed results are in very good agreement with measurements close to the East and West walls, but generally underestimate measurements on the North wall, where there is a large scatter in data reported from reference points located on Vassar St. and on the South Wall where close proximity of the Building 57 make reliable interpretation difficult.

Subsurface vertical displacements were also measured by magnet extensometers in a borehole located close to the South wall (Fig. 1). Figure 13 compares the computed and measured vertical heave at three elevations within the BBC (the deepest at El. -18.6 m is located 3.3m below the toe of the diaphragm wall, Fig. 3). Heave occurs at all three elevations through the end of excavation (April 2001), and stabilizes immediately after casting of the mat foundation. Although the analyses are

generally in good agreement with maximum heave measured at El. -9.4m, the results are much less consistent for the other two extensometers (i.e., heave underestimated at El. -15.5m and overestimated at El. -18.6m). The data scatter and close correspondence in displacements at El's. -9.4m and -15.5m suggest limitations in the reliability of the measured data. The computed results again show small differences in undrained analyses performed using the MC and MIT-E3 soil models (Case A vs Case B). The inclusion of partial drainage (Case C) clearly affects the response predicted close to the top of the clay (El. -9.4m) and generates better agreement with the extensometer data at this elevation.

Figure 14 shows similar comparisons between computed and measured pore pressures at two elevations within a borehole located near the center of the excavation (Fig. 1). The piezometers show a maximum drawdown of approximately 20m in piezometric head for excavation down to final grade (March-April 2001), corresponding to a pore pressure ratio, $\Delta u/\Delta\sigma_v \approx 0.8$. This result is consistent with 3D stress changes associated with the footprint of the excavation. There is a small recovery in piezometric head due to casting of the mat foundation ($\Delta H = +2.5$m) by June 2001. The numerical analyses in very good agreement with measured pore pressures during early stages of the excavation (through mid February), but underestimate the drawdown during March. This result reflects approximations in the modeling of berm removal during this time period. It is interesting to note that Case B predicts smaller drawdown than Case A, during later stages of excavation at El. -15.2m. This reflects the simulation of shear induced pore pressures for undrained shearing using the MIT-E3 soil model, and produces larger deviations from the measured behavior. However, when partial drainage is included (Case C) the behavior is coincidentally much closer to the MC model (Case A).

CONCLUSIONS

The three-dimensional finite element analyses described in this paper were made practical through recent advances in computational capabilities including the formulation of embedded pile elements (for modeling tieback-soil interactions) and robust multicore, iterative solvers (that are far more efficient that direct solvers for large FE models) in the Plaxis 3D program ('Picos'; Brinkgreve et al., 2011). This paper has demonstrated the predictive capabilities of 3D FE analyses for the excavation and

support of the Stata Center basement, a project completed more than 12 years ago. The analyses are able to explain many features of the observed performance including differences in diaphragm wall deformations associated with sections supported by tieback anchors, raker beams and corner bracing using a simple elasto-plastic soil model (Mohr-Coulomb model), assuming undrained conditions in the underlying BBC. Analyses using a more complex soil model (MIT-E3) and accounting for partial drainage (i.e., coupled consolidation) over the 200 day timeframe of excavations have only secondary effects on the predicted performance, but provide important insights to understand the computed behavior.

The analyses clearly show that tiebacks anchored within the upper layers of BBC, were only partially effective in constraining wall and ground deformations. Further refinements of the FE model are needed to understand how uncertainties in the stratigraphy and properties of adjacent building foundations affect the predicted performance of the excavation support system. Credible predictions are an essential step towards use of numerical analyses in designing excavation support systems that mitigate impacts on adjacent structures.

ACKNOWLEDGMENTS

The Stata Center was designed by Gehry Partners and constructed by Beacon-Skanska Construction Company. Haley and Aldrich were the geotechnical consultants responsible for site investigation, design of field instrumentation and monitoring of the basement construction. The views and opinions expressed in this paper are those of the Authors and not represent those of the organizations or other individuals responsible for completion of this project. The Authors are grateful to former MIT Provost Robert Brown for supporting the original research project that enabled documentation of the project, to David Lewis who oversaw the project for the MIT Department of Facilities, and to Robert Hewitt and Rebecca Brown (H&A) for their very helpful collaboration during construction. The first Author (ZYO) was supported by a Bolashak Scholarship from the Republic of Kazakhstan during his SM studies at MIT.

REFERENCES

Berman, D.R., Germaine, J.T., and Ladd, C.C. (1993) "Characterization of engineering properties of Boston Blue Clay for the MIT campus." Research Rept. 93-16, Dept. of Civil & Environ. Eng., MIT, 146p.

COI (2005) "Report of the Committee of Inquiry into the incident at the MRT Circle Line worksite that led to collapse of Nicoll Highway on 20th April, 2004," Ministry of Mnapower, Singapore.

Corral, G. (2013). "Methodology for Updating Numerical Predictions of Excavation Performance." *Sc.D. Thesis, Department of Civil and Environmental Engineering, Cambridge, MIT*. 515p.

Dong, Y., Burd, H., Houlsby, G.T. & Xu, Z. (2013) "3D FEM modeling of a deep excavation case history considering small strain stiffness of soil and thermal shrinkage of concrete," *Proc. 7th Intl. Conf. on Case Histories in Geotechnical Engineering*, Chicago, #3.28b.

Finno, R.J., Blackburn, J.T. & Roboski, J.F. (2007) "Three-dimensional effects for supported excavations in clay," *ASCE Journal of Geotechnical and Geoenvironmental Engineering*, 133(1), 30-36.

Haley & Aldrich, (2000) "Report on geotechnical investigations and foundation design recommendations for the Ray and Maria Stata Center, Massachusetts Institute of Technology Cambridge, Massachusetts," submitted to MIT and Beacon-Skanska Construction Company.

Hewitt, R.D. & Haley, M.X. (2003) "Stata Center, Deep excavation meets MIT's needs," Structure Magazine, December, 4p.

Hewitt, R.D., Haley, M.X. & Kinner, E.B. (2003) "Case history of deep excavation on an urban campus," *Proc. Soil & Rock America 2003 (12th Pan-American Conference on Soil Mechanics and Geotechnical Engineering),* Glückauf, 2, 1997-2005.

Houlsby, G.T. (1999) "A model for the variable stiffness of undrained clay," *Proc. Intl. Symp. Pre-Failure Deformations of Soil*, Torino, 1, 443-450.

Jen, L. C. (1998), "The design and performance of deep excavations in clay." *PhD Thesis. Department of Civil and Environmental Engineering, Cambridge, MIT*, 698p.

Ladd, C.C., Young, G.A., Kraemer, S.R. and Burke, D.M. (1999) "Engineering properties of Boston Blue Clay from Special Testing Program." *Proceedings, Special Geotechnical Testing: Central Artery/Tunnel Project in Boston, Massachusetts*, ASCE GSP 91, GeoCongress '98, National Convention, Boston, 1-24.

Ladd, C.C. & DeGroot, D.J. (2003) Recommended practice for soft ground site characterization – Arthur Casagrande Lecture), *Proc. Soil & Rock America 2003 (12th Pan-American Conference on Soil Mechanics and Geotechnical Engineering),* Glückauf, 1, 3-58.

Lee, F.H., Yong, K.Y., Quan, K.C.N. & Chee, K.T. (1998) "Effects of corners in strutted excavations," *ASCE Journal of Geotechnical and Geoenvironmental Engineering*, 124(4), 339-349.

Lee F.H., Hong, S.H., Gu Q. & Zhao, P. (2011) "Application of large three-dimensional finite-element analyses to practical problems," *ASCE Intl. J. Geomechanics*, 11(6), 529-539.

Olsen, M.B. (2001) "Measured performance of a large excavation on the MIT campus," SM Thesis, Department of Civil and Environmental Engineering, Massachusetts Institute of Technology, Cambridge, MA, 275p.

Ou, C.Y., Chiou, D.C. & Wu, T.S. (1996) "Three-dimensional finite element analysis of deep excavations," *ASCE Journal of Geotechnical Engineering*, 122(5), 337-345.

Brinkgreve, R.B.J., Engin, E. & Swolfs, W.M. (Eds) (2012) "Plaxis 3D 2011," Balkema.

Rodriguez, D.W. (2000) "Project time-lapse," Unpublished UROP report submitted to CSAIL Computer Graphics Group, MIT.

Sadek, M. & Shahrour, I. (2004) "A three dimensional embedded beam element for reinforced geomaterials," *Intl. J. for Numerical and Analytical Methods in Geomechanics*, 28(9), 931-946.

Simpson, B. (1992) "Retaining structures – displacement and design (32nd Rankine Lecture)," *Géotechnique*, 42(4), 539-576.

Taylor, D.W. (1944) "An unusual foundation problem the alumni pool building," *J. of the Boston Society of Civil Engineers*, 31(4); republished in *Contributions to Soil Mechanics, 1941-1953*, Boston Society of Civil Engineers, 136-146.

Ukritchon, B., Whittle, A.J. & Sloan, S.W. (2003). "Undrained stability of braced excavations in clay," *ASCE Journal of Geotechnical and Geoenvironmental Engineering*, 129(8), 738-756.

Whittle, A.J. & Kavvadas, M.J. (1994). "Formulation of the MIT-E3 constitutive model for overconsolidated clays," *ASCE Journal of Geotechnical Engineering*, 120(1), 173-199.

Whittle, A.J., DeGroot, D.J., Ladd, C.C. & Seah, T-H. (1994). "Model prediction of the anisotropic behavior of Boston Blue Clay," *ASCE Journal of Geotechnical Engineering*, 120(1), 199-225.

Whittle, A.J., Sutabutr, T., Germaine, J.T. & Varney, A. (2001) "Prediction and interpretation of pore pressure dissipation for a tapered piezoprobe," *Géotechnique*, 51(7), 601-617.

Whittle, A.J. & Davies, R.V. (2006). "Nicoll Highway Collapse: Evaluation of geotechnical factors affecting design of excavation support system," *International Conference on Deep Excavations*, Singapore, 16p.

Yeow, H.C., Pillai, A.K. & Wallace, J. (2006) "The use of a full non-linear 3D finite element model n ground movement and risk assessment in a major infrastructure project," *Proc. ASCE GeoCongress*, 6p.

Zdravkovic, L., Potts, D.M. & StJohn, H.D. (2005) "Modelling of a 3D excavation in finite element analysis," *Géotechnique*, 55(7), 497-513.

1

2 **Appendix A. MIT-E3 model input parameters (Whittle et al., 1994)**

Laboratory Test	Description	Parameter	Boston Blue Clay
One-dimensional Compression	Reference Void Ratio on VCL	e_0	0.988
	Normally Consolidated Compression	λ	0.184
	Non-linear Volumetric Swelling Behavior	C	22.0
		n	1.6
	Irrecoverable Plastic Strain	h	0.2
K_0 –oedometer or K_0 -Triaxial	K_0 for virgin normally consolidated clay	K_{0NC}	0.534
	Poisson's Ratio	2G/K	1.05
Undrained Triaxial Shear Tests	Critical State Friction Angles in Triaxial Compression and Extension	φ'_{TC}	33.4^0
		φ'_{TE}	45.9^0
OCR=1; CK_0UC	Undrained Shear Strength (geometry of bounding surface)	c	0.866
	Amount of Post-peak Strain Softening in Undrained Triaxial Compression	s_t	4.5
OCR=1; CK_0UE	Non-linearity at Small Strains in Undrained Shear	ω	0.07
OCR=2; CK_0UC	Shear Induced Pore Pressures for OC Clay	γ	0.5
Shear Wave Velocity	Small strain compressibility at load Reversal	κ_0	0.001
Drained Triaxial	Rate of Evolution of Anisotropy (rotation of bounding surface)	Ψ_0	100.0

Building	No. Storeys (+ basements)	Foundation Type	El. (m CCB[1])	Notes
36	9 + 2 concrete	Mat	-0.6	Fairchild Building
26	5 + 1 concrete	Footings	+0.3	Compton Labs.
70	8 + 1	PIF's	-1.9	Parking garage (subsequently demolished)
57	3+pool	Caissons 0.9 m dia. 3.0m underream	-1.9	Alumni Pool Ave. net surcharge on clay: Δq = 145kPa

Note: 1. Cambridge City Base, CCB = MSL – 3.3m

Table 1. Foundations of adjacent buildings

Wall	Level	Number of tiebacks	Pre-Stress (kN)	Free Length (m)	Bond Length (m)
South	1	45	498	15	12
	2	"	569	6	15
	3	"	569	3	15
East	1	25	498	15	12
	2	"	569	6	15
	3	"	569	3	15
West	1	25	498	15	12
	2	"	569	6	15
	3	"	569	6	15

Note: All anchors - 4# strand, 1.52cm, Grade 270 steel, EA = 1.46×10^5 kN, inclined at 20°

a) Tieback anchors

North Wall	No. struts	Top El. (m CCB)	Pre-Load (kN)	Length (m)	Diameter, (cm)	Wall Thickness (cm)	EA (kN)
Level 1	8	+3	1446	27	91	1.32	6.15×10^6
Level 2	8	-3	2357	26	91	2.04	1.21x107

b) Raker beams

Corner	Level & [No.]	Lengths (m)	Ave. Pre-Load (kN)	Wall Thickness (cm)
NW	1 [3]	12.4, 23.3, 36.0	1870	1.0, 1.0, 1.0
	2 [3]	"	3110	1.3, 1.3, 1.6
SW	1 [2]	11.5, 22.3	1530	1.0, 1.0
	2 [2]	"	2590	1.3, 1.3
NE	1 [3]	11.5, 22.3, 33.1	2050	1.0, 1.0, 1.0
	2 [3]	"	3460	1.3, 1.3, 1.6
SE	1 [4]	6.1, 16.9, 27.7, 36.9	3350	1.0, 1.0, 1.0, 1.0
	2 [4]	"	4690	1.0, 1.6, 1.3, 1.0

All struts: Pipe section 0.91m dia.

c) Corner struts

Table 2. Properties of structural support elements

Unit	Top El. (m)	Model	γ_t (kN/m^3)	s_u	ϕ' (°)	OCR	K_0	G/σ'_{v0}	ν'	k (m/day)
Granular Fill	6.4	MC (D)	18.9	--	35	--	0.50	75	0.3	0.9
Organics	3.0	MC (UD)	15.7	48	--	--	0.5	150	0.3	0.09
Marine Sand	1.2	MC (D)	20.4	--	37	--	0.5	230	0.3	0.09
BBC (Upper)	-3.0	MC (UD)	18.4	68 61	--	--	0.8	75	0.3	$4x10^{-5}$
BBC (Lower)	-17.0	MC (UD)	19.3	61 93	--	--	0.6	75	0.3	$4x10^{-5}$
Glacial Till	-29.0	MC (D)	22.0	0	43	--	1.0	385	0.3	0.009

a) Mohr-Coulomb Model (MC)

Unit	Top El. (m)	Model	γ_t (kN/m^3)	s_u (kPa)	OCR	K_0	G/σ'_{v0}	ν'	k (m/day)
BBC	-3.0	MIT-E3	18.4	Appendix A	2.6	0.78	Appendix A		$4x10^{-5}$
	-6.4			s_{uDSS}	2.1	0.70			
	-9.1			matches	1.7	0.64			
	-12.2			Fig. 4c	1.4	0.59			
	-16.8				1.25	0.57			

b) MIT-E3 soil model used in analyses Cases B and C

Table 3. Input parameters for soil models

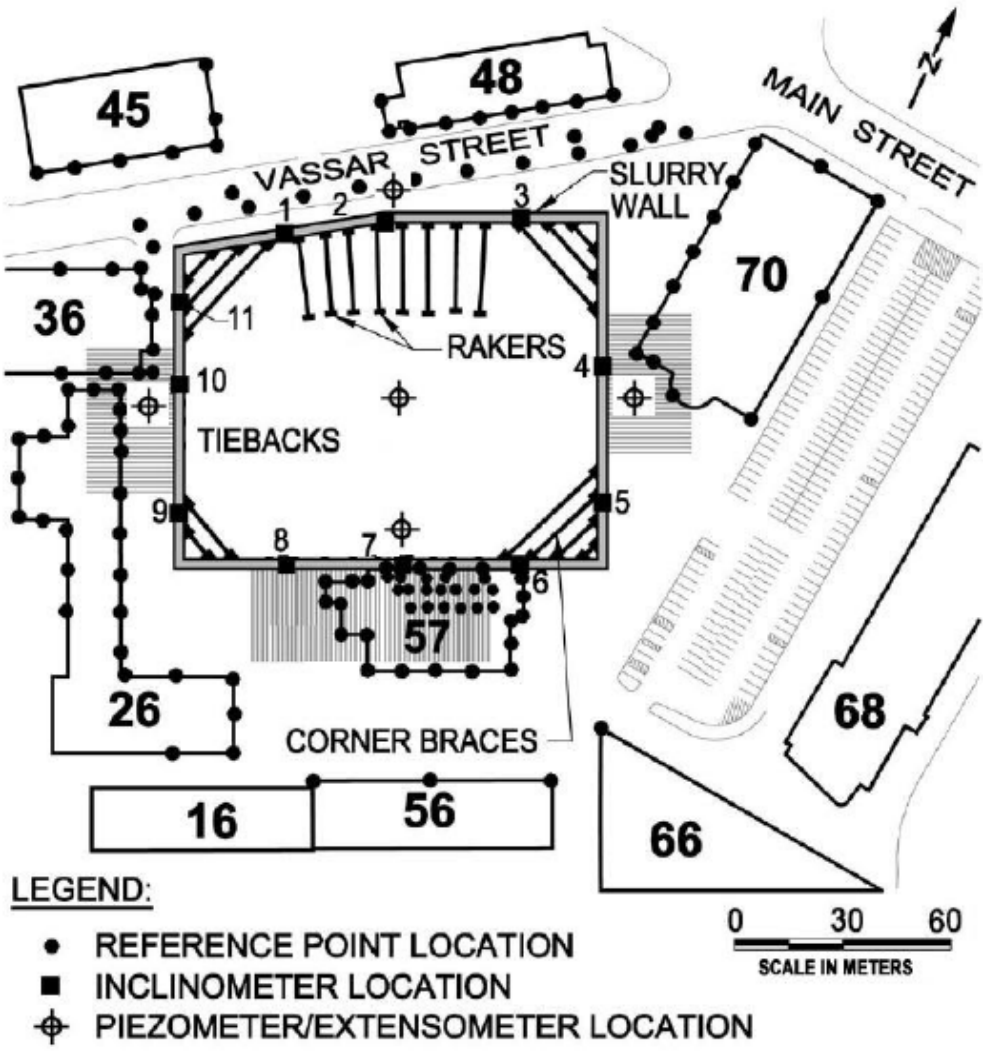

Figure 1. Plan of Stata Center basement, adjacent buildings and monitoring locations (adapted from Hewitt et al., 2003)

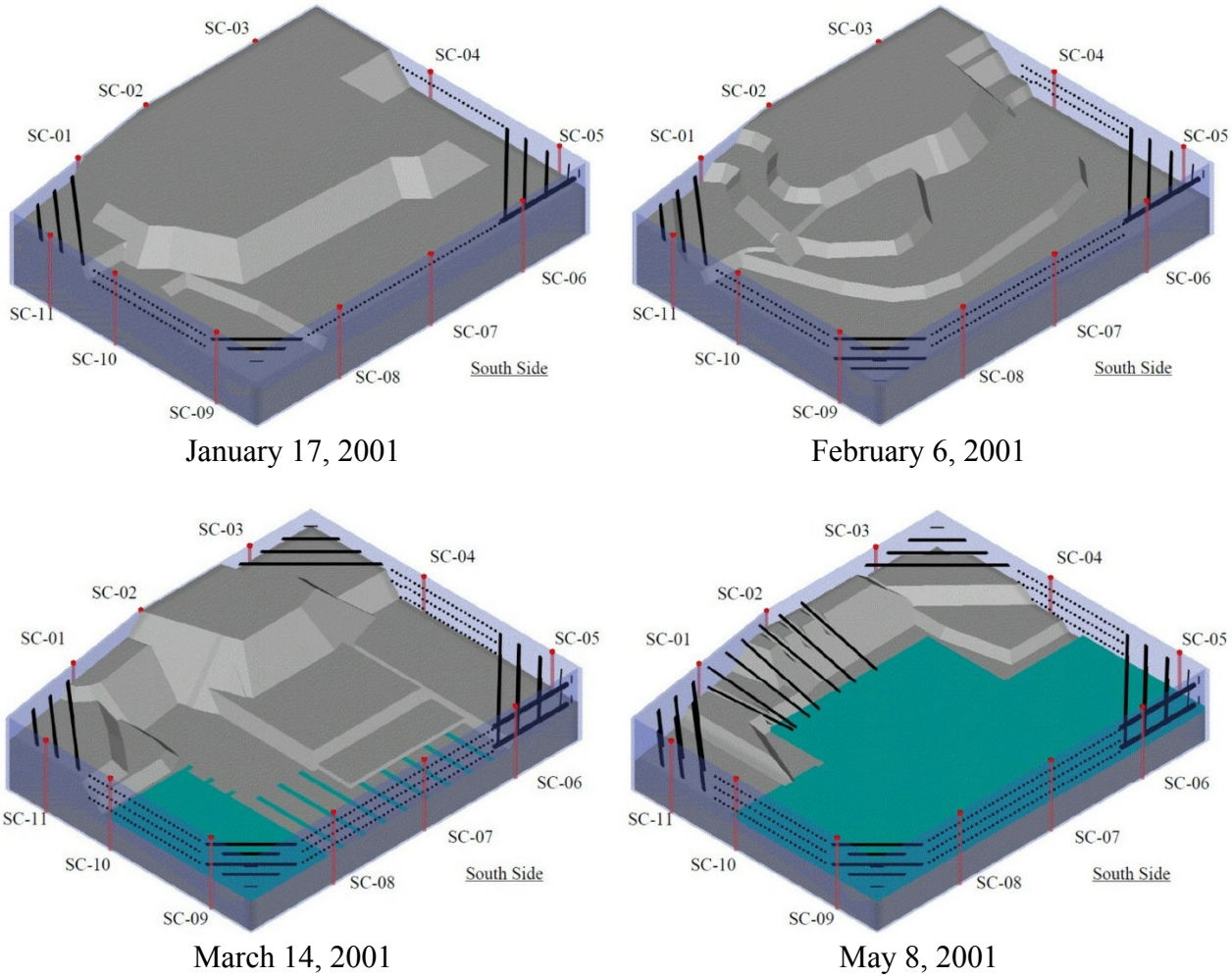

Figure 2. Schematic diagrams of excavation support at four stages of construction (Olsen, 2001)

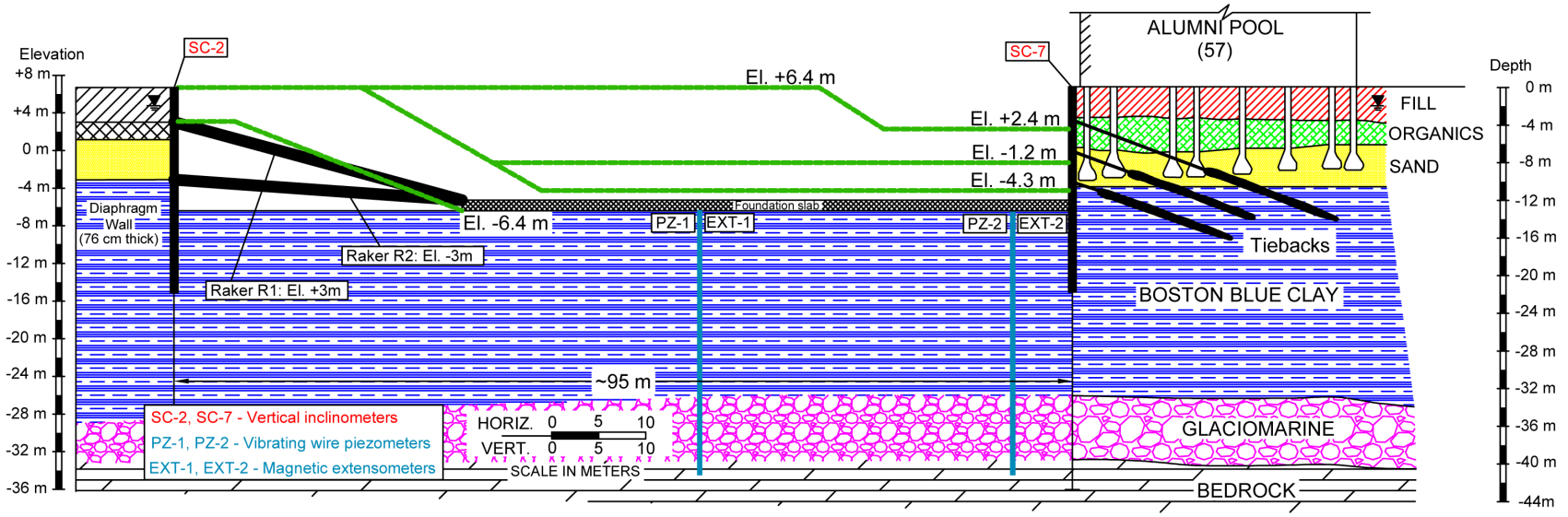

Figure 3. Typical N-S cross-section for Stata basement excavations showing support systems, soil profile and foundations of Alumni Pool (Building 57)

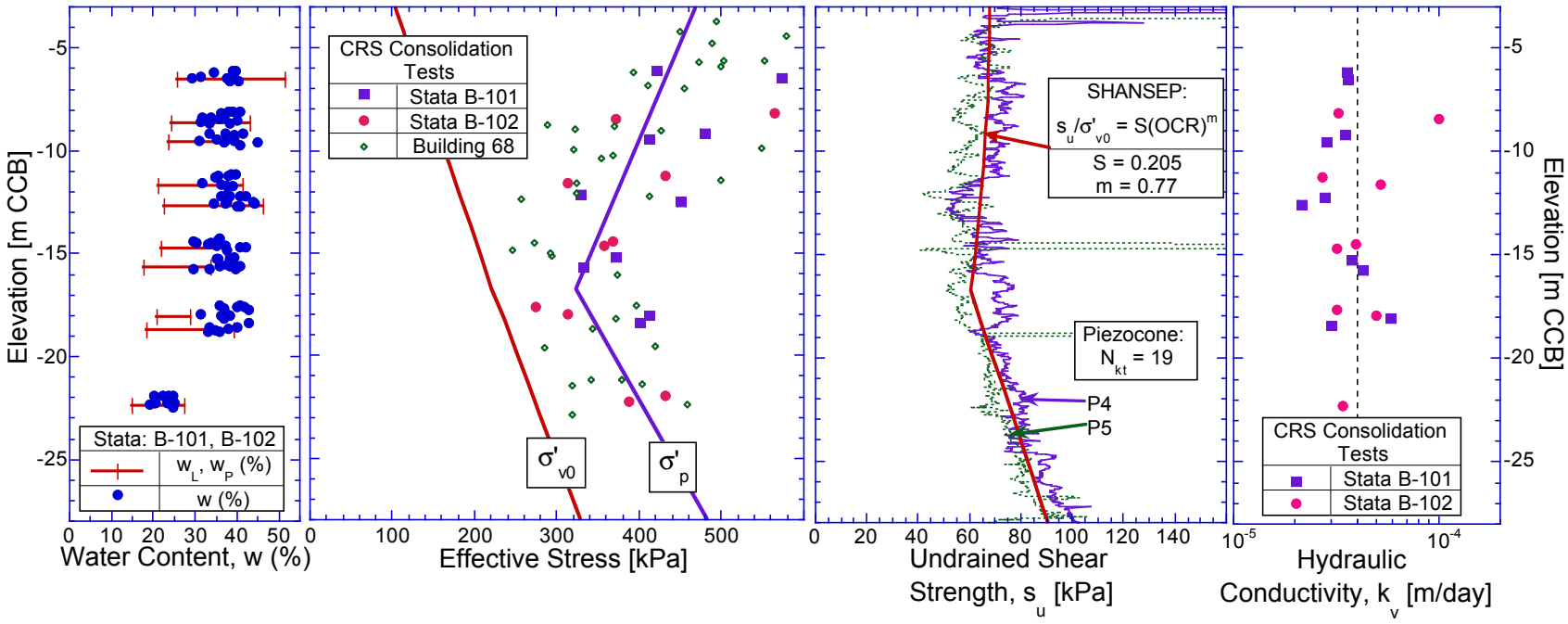

Figure 4. Properties of BBC at Stata Center site

Figure 5. Photos illustrating installation of
a) tieback anchors (2nd row East wall) and b) raker struts (1st level North wall)

Actual Project phases				Calendar plan							
Description	**Start Date**	**End Date**	**Duration**	November	December	January	February	March	April	May	June
Diaphragm Wall installation	July, 2000	November, 2000	~150 days								
First Level of West Tiebacks	12/05/00	12/27/00	22 days								
First Level of South-West Bracing	12/06/00	12/13/00	7 days								
First Level of South Tiebacks	12/21/00	01/05/01	15 days								
First Level of South-East Bracing	12/18/00	01/05/01	18 days								
First Level of East Tiebacks	01/02/01	01/09/01	7 days								
First Level of North-West Bracing	01/08/01	01/17/01	9 days								
Second Level of West Tiebacks	01/02/01	01/18/01	16 days								
Second Level of South Tiebacks	01/12/01	01/23/01	11 days								
Second Level of East Tiebacks	01/23/01	02/01/01	9 days								
Second Level of South-West Bracing	01/22/01	01/29/01	7 days								
Third Level of West Tiebacks	01/29/01	02/09/01	11 days								
Third Level of South Tiebacks	02/02/01	02/20/01	18 days								
Second Level of South-East Bracing	02/02/01	02/16/01	14 days								
Third Level of East Tiebacks	02/21/01	03/26/01	33 days								
First Level of North-East Bracing	03/06/01	03/14/01	8 days								
Second Level of North-West Bracing	04/25/01	05/01/01	6 days								
Foundation slab at the center	03/03/01	04/25/01	53 days								
First Level of Raker support	04/06/01	05/15/01	39 days								
Second Level of Raker support	05/09/01	06/01/01	23 days								
Second Level of North-East Bracing	05/30/01	06/06/01	7 days								
Excavation process	11/14/00	06/19/01	~219 day								
Date				Nov 14	Dec 5	Dec 13	Dec 19	Dec 27	Jan 6	Jan 11	Jan 17
				Jan 29	Feb 2	Feb 6	Feb 13	Feb 20	Mar 14	Mar 24	Apr 6
				Apr 25	May 1	May 8	May 17	Jun 1	Jun 6		
Phase #				02	03	05	07	09	13	16	18
				21	27	28	29	30	33	34	35

Figure 6. Schedule of construction activities for State Center basement

a) Photograph (Nov. 28 from Building 26)

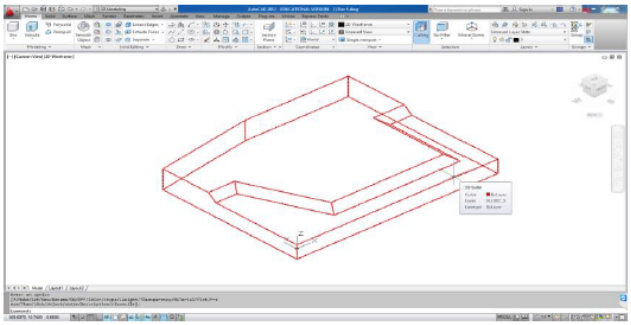

c) CAD model

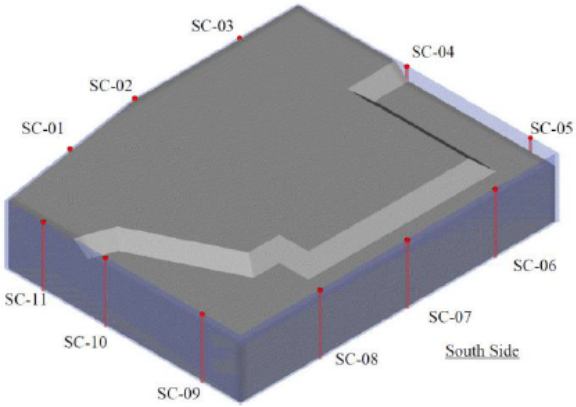

b) Geometric model – Dec 5th 2000 (Olsen, 2001)

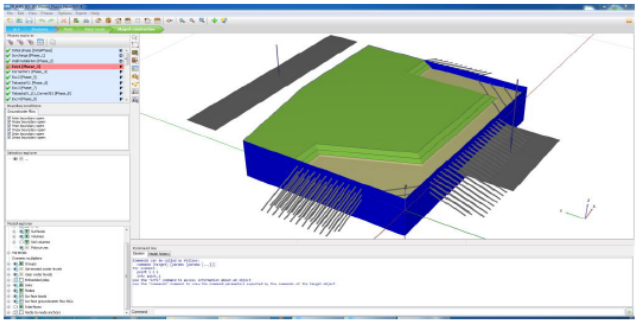

d) FE model of excavation and supports

Figure 7. Development of 3D finite element model of construction history

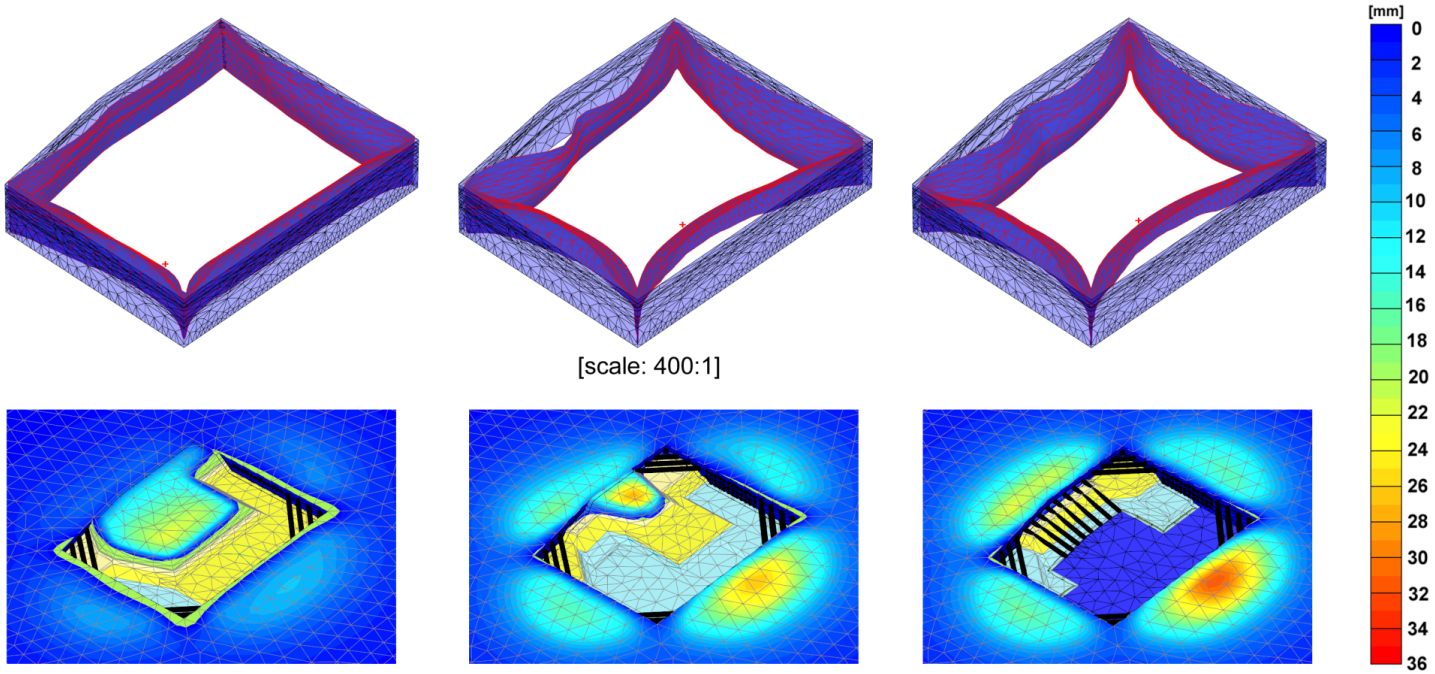

a) Stage 13 (Jan. 17, 2001) c) Stage 27 (March 14, 2001) d) Stage 30 (May 8, 2001)

Figure 8. Typical predictions of wall deflections and surface settlements from base Case A

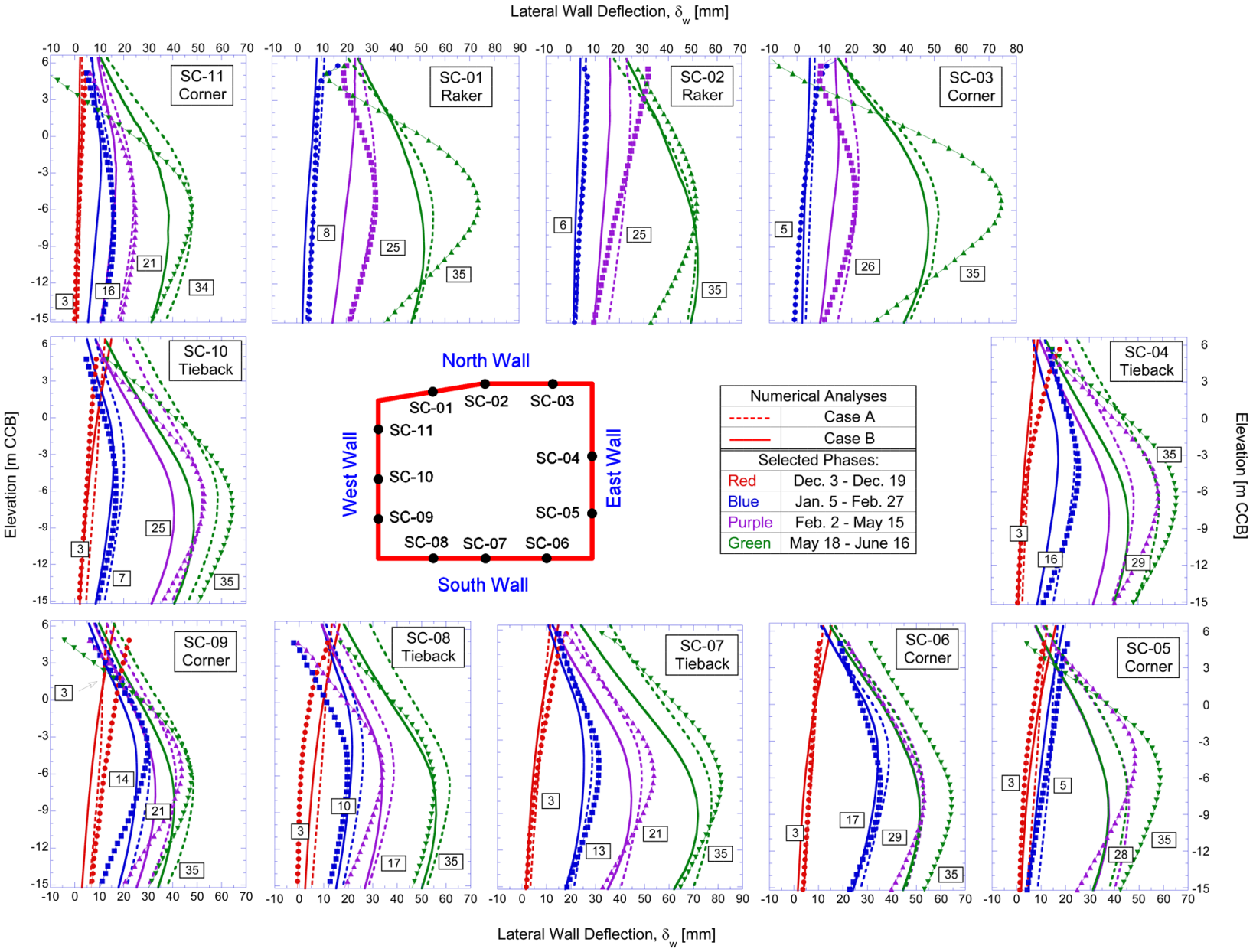

Figure 9. Comparison of computed and measured lateral wall deflections at selected phases of construction based on undrained analyses and comparing different soil models for BBC (symbols – measured data)

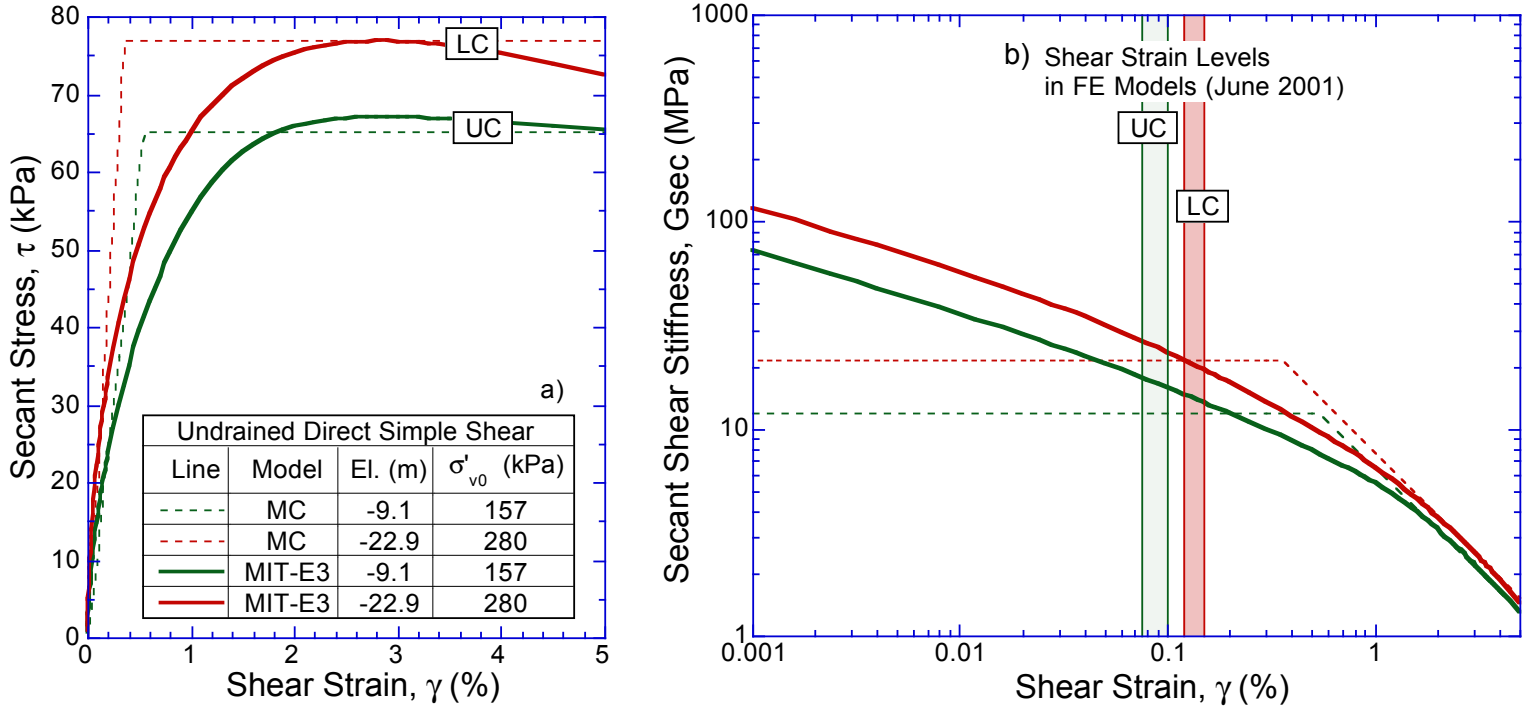

Figure 10. Comparison of stiffness properties for Upper (UC) and Lower (LC) Units of BBC using EPP and MIT-E3 soil models a) undrained simple shear tests; b) comparison with shear strains from FE models

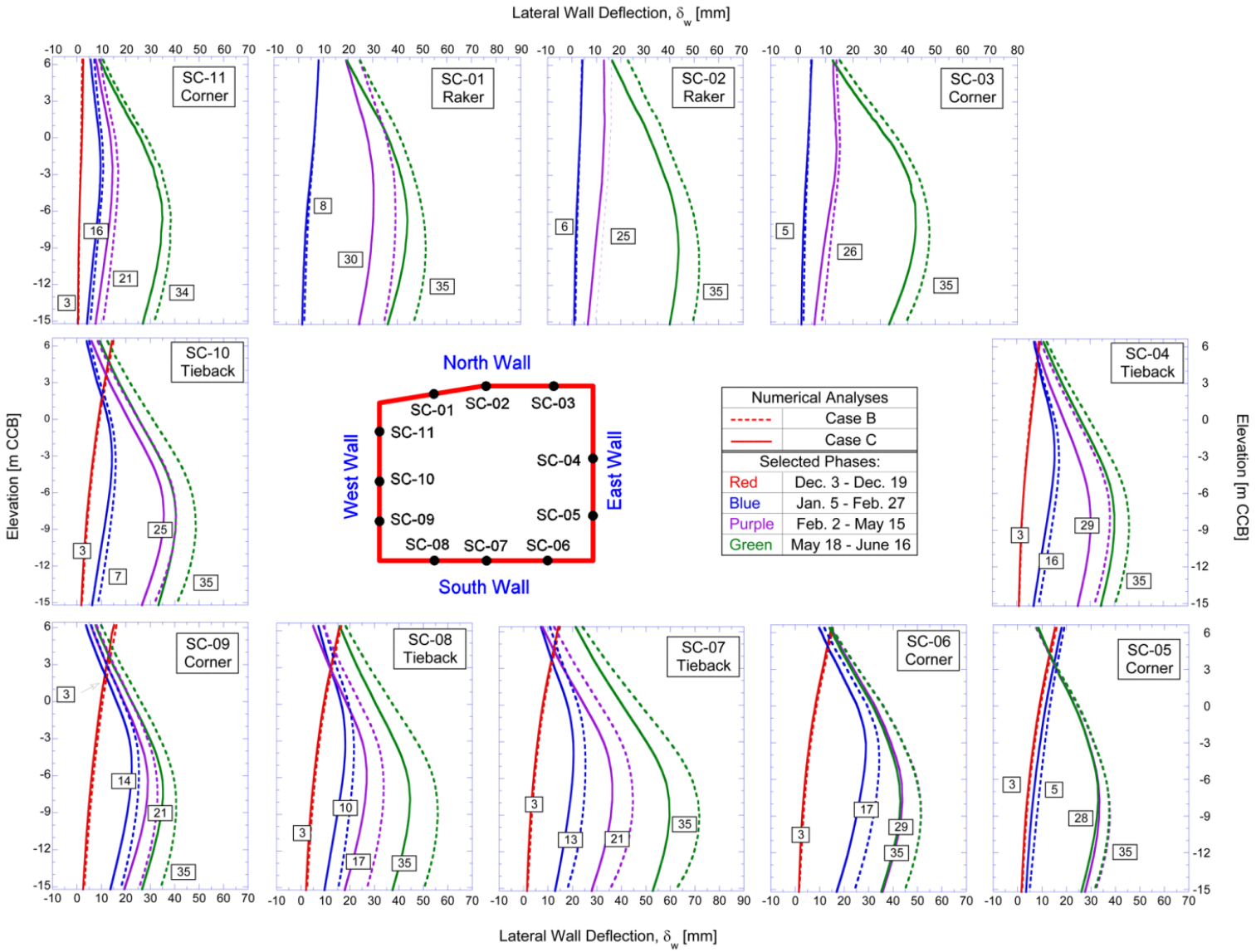

Figure 11. Effect of partial drainage on predicted wall deflections

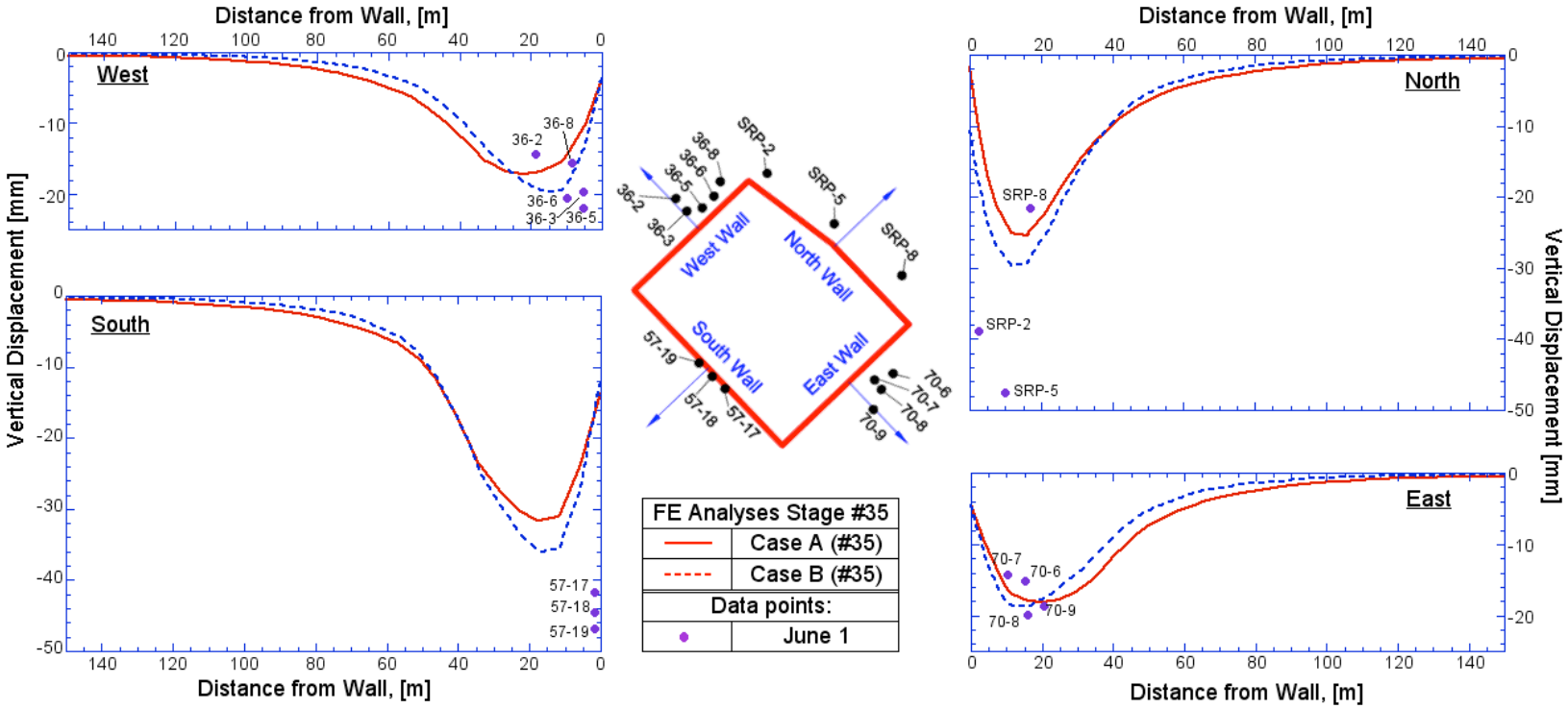

Figure 12. Comparison of computed and measured settlements at the end of excavation

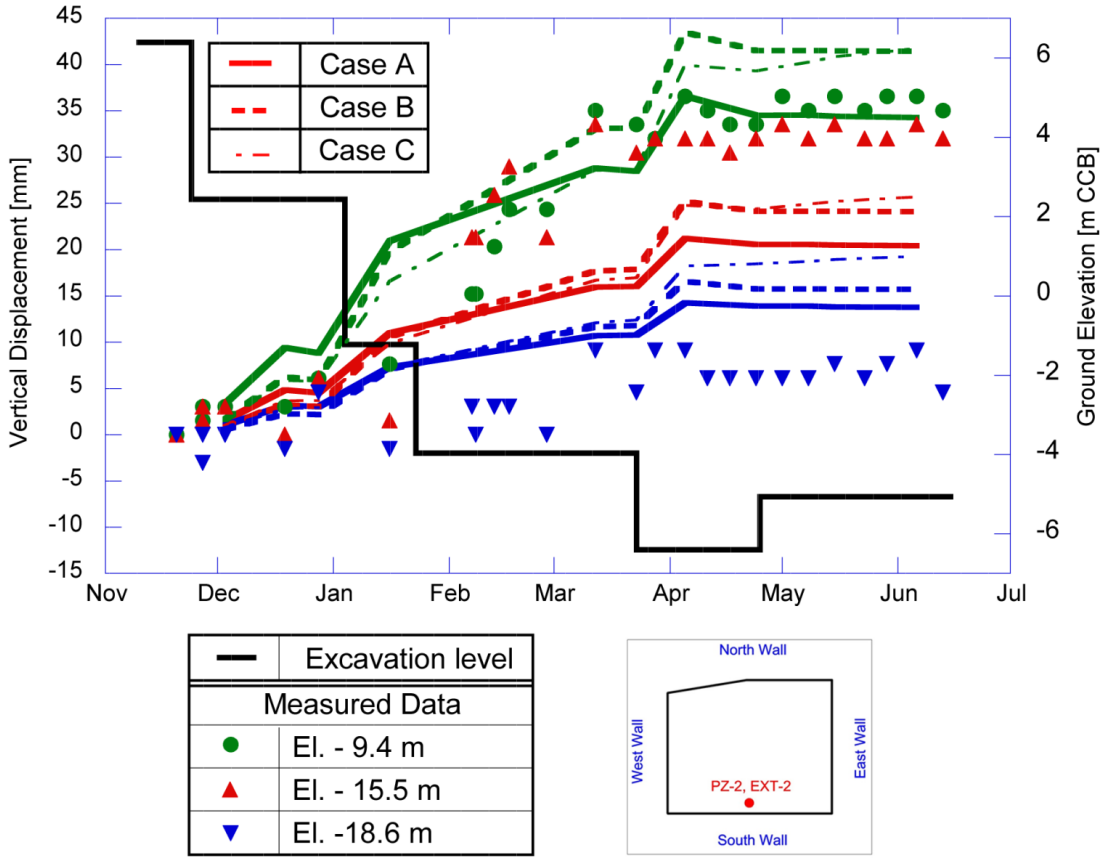

Figure 13. Comparison of predicted and measured heave in clay below base of excavation

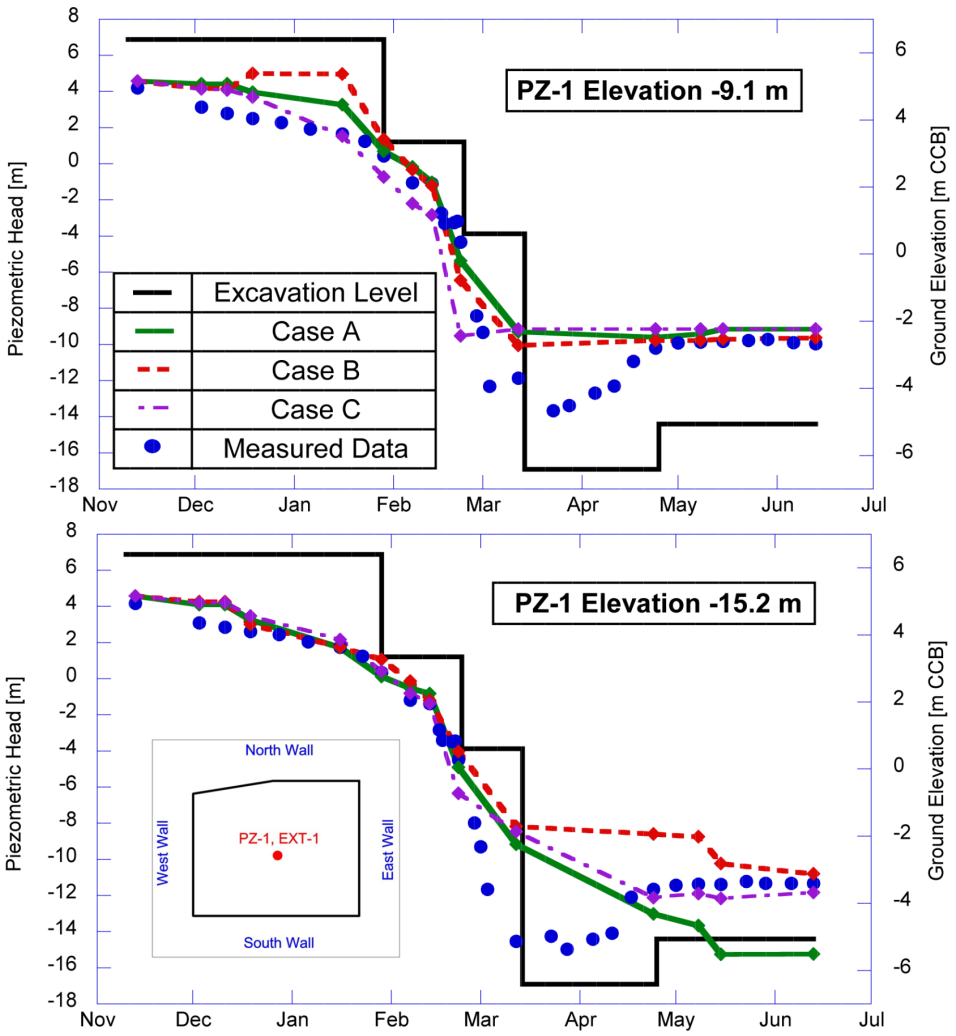

Figure 14. Comparison of predicted and measured piezometric head in clay beneath center of excavation